Low Temperature Thermodynamical Properties of the Organic Chain Conductor (TMTTF)2Br

J. Lasjaunias, P. Monceau, D. Starešinić, K. Biljaković, J. Fabre

Low Temperature Thermodynamical Properties of the Organic Chain Conductor $(TMTTF)_2Br$

J.C. Lasjaunias ([1,*]), P. Monceau ([1]), D. Starešinić ([2,1]), K. Biljaković ([2,1]) and J.M. Fabre ([3])

([1]) CRTBT-CNRS, associé à l'UJF, BP 166, 38042 Grenoble Cedex 9, France
([2]) Institute of Physics, PO Box 304, HR-1000 Zagreb, Croatia
([3]) Laboratoire de Chimie Organique Structurale, Université des Sciences et Techniques du Languedoc, 34060 Montpellier, France

(Received 30 April 1997, revised 15 July 1997, accepted 23 July 1997)

PACS.05.70.Ln – Non equilibrium thermodynamics, irreversible processes
PACS.75.30.Fv – Spin-density waves
PACS.71.45.Lr – Charge-density-waves systems

Abstract. — We report on the first thermodynamical investigation of $(TMTTF)_2Br$ in its antiferromagnetic ground state. There is a discontinuity in the lattice specific heat, C_p/T^3, at 1.9-2.0 K which seems to reflect the existence of the Spin Density Wave (SDW) sub-phase. This discontinuity is similar to those we have measured in other quasi one-dimensional organic salts of the Bechgaard family. Above 2.5 K there is another anomaly which we attribute either to a pure vibrational lattice origin or/and to an additional configurational entropy, a manifestation of the disordered SDW ground state coupled to the lattice. As for a broad variety of density wave compounds, the specific heat of $(TMTTF)_2Br$ exhibits a contribution of low-energy excitations. They are at the origin of the time-dependent specific heat and complex energy-relaxation dynamics below 1 K. However, the corresponding time scale is much shorter than in the case of $(TMTSF)_2PF_6$, the Incommensurate SDW compound. We tentatively ascribe the difference in the kinetics of the energy relaxation of $(TMTTF)_2Br$ and $(TMTSF)_2PF_6$ to the different degrees of commensurability of their ground states.

Résumé. — Nous décrivons la première caractérisation thermodynamique de $(TMTTF)_2Br$ dans son état fondamental antiferromagnétique. Une discontinuité dans la chaleur spécifique du réseau en C_p/T^3 apparaît à 1,9-2,0 K, qui semble refléter l'existence d'une sous-phase de l'Onde de Densité de Spin (ODS). Cette discontinuité est similaire à celle déjà mesurée dans d'autres sels organiques quasi-1D des composés de Bechgaard. Au-dessus de 2,5 K apparaît une nouvelle anomalie en C_p/T^3 que l'on attribue soit à une origine purement vibrationelle, ou/et à une contribution d'entropie de configuration, manifestation du désordre de l'onde de densité dans son état de base en couplage au réseau. Comme pour une large variété de composés à onde de densité, la chaleur spécifique de $(TMTTF)_2Br$ présente une contribution d'excitations de faible énergie, qui sont à l'origine de la dépendance en temps de la chaleur spécifique et de la dynamique complexe de relaxation d'énergie en dessous de 1 K. Toutefois l'échelle des temps correspondante est beaucoup plus faible que dans le cas du composé à ODS incommensurable $(TMTSF)_2PF_6$. Nous proposons pour origine de la différence des cinétiques de relaxation d'énergie entre $(TMTTF)_2Br$ et $(TMTSF)_2PF_6$ la différence de l'approche à la commensurabilité de leurs états de base.

(*) Author for correspondence (e-mail: lasjau@labs.polycnrs-gre.fr)

1. Introduction

The organic chain-like compounds of general formula $(TMTSF)_2X$ (where TMTSF: tetramethyltetraselenafulvalene contains Se atoms) and $(TMTTF)_2X$ (where TMTTF: tetramethyltetrathiafulvalene contains S atoms) with X being a mono-anion PF_6, AsF_6, Br, NO_3, ClO_4, ... are model systems for the investigation of the fundamental properties of quasi-one-dimensional systems [1–3]. Different Ground States (GS) can be formed as the effective dimensionality of the conduction electrons is highly sensitive to small changes in temperature, pressure or magnetic field. The selenium salts, or Bechgaard salts, are metallic at room temperature down to low temperature where their phase diagram exhibits Spin Density Waves (SDW), superconductivity and magnetic field dependent phenomena. The difference between the $(TMTTF)_2X$ and $(TMTSF)_2X$ salts is largely attributed to the difference in the on-site Coulomb repulsion. A $4k_F$ charge localisation of Mott-Hubbard type occurs in the $(TMTTF)_2X$ salts in the range 100-200 K, leaving unaffected the spin degrees of freedom. Interchain exchange interaction between one-dimensional $2k_F$ spin fluctuations stabilizes a three dimensional antiferromagnetic (AF) ordering. In $(TMTTF)_2Br$ this SDW transition occurs at $T_{AF} \sim 11$ K-13 K as revealed in the anisotropy of the static magnetic susceptibility, the existence of antiferromagnetic resonance below T_N, the divergence of the proton ^1H nuclear relaxation T_1^{-1} [2]. Characteristic line shapes obtained by ^{13}C NMR [4] at ambient pressure have been offered as the evidence of antiferromagnetism GS commensurate with the lattice (C-SDW). In contrast, the NMR line shapes of $(TMTSF)_2X$ salts show the characteristics of an Incommensurate SDW (I-SDW) below $T_{SDW} = 12$ K [4,5]. It was shown that the SDW in $(TMTTF)_2Br$ becomes incommensurate under a modest pressure (~ 5 kbars) when the charge gap is suppressed [6]. Recent X-ray investigation on Se and S compounds give more informations about the nature of their magnetic ground states; they show the existence of charge density modulation in their magnetic phases. $(TMTSF)_2PF_6$ exhibits a $2k_F$ mixed CDW-SDW modulation [7,8] and $(TMTTF)_2Br$ a $4k_F$ CDW, probably set in by magnetoelastic coupling of the lattice degrees of freedom with the AF modulation [8].

Incommensurate spin/charge density wave systems exhibit spectacular collective transport properties. Non-linear conductivity occurs above a sharp threshold field (which in the case of I-SDW is in the range of a few mV/cm) when the density wave is depinned from impurities. The DW ground state is characterized by disorder induced by the frozen metastable states which result from the interaction between the DW phase and the randomly distributed impurities. This disorder is the best revealed in low temperature thermodynamical measurements: they show additional low-energy excitations to regular phonon which contribute to the specific heat below $T \sim 0.5$ K according to a law $C_p \sim T^\nu$ with $\nu < 1$, and non-exponential enthalpy relaxation with "aging effects" which prove the non-linearity of the specific heat in this T-range and reveal the broad distribution of relaxation times for recovering the thermodynamical equilibrium. All these properties have been observed recently in the I-SDW compound $(TMTSF)_2PF_6$ [9].

Hereafter we report on the low-T thermodynamical properties of C−SDW $(TMTTF)_2Br$ and compare them with those obtained in $(TMTSF)_2PF_6$ with the aim to find the role of commensurability in the Low-Energy Excitations (LEE) and the relaxational mechanism in their C-SDW and I-SDW ground states. As in the previous study of $(TMTSF)_2PF_6$ [9], we have performed a systematic study of thermodynamical properties under various durations of the energy delivery, from pulse of $\sim$ 0.2-0.3 s up to 10 hours. The time-dependence effects are manifested in two ways: the most obvious appears as the progressive deviation from an exponential decay of the thermal transient in response to a heat pulse, on lowering T: this occurs around 0.7 K. Simultaneously, C_p deviates from the T^3 regime of the lattice contribution,

and reveals the increasing part of the LEE contribution, at the origin of the slow dynamics in the thermal response. The second property is the dependence of the transients with the duration of heat delivery — that we have named "aging" — [10], the consequence of which yields a time-dependent specific heat.

2. Experimental

Crystals of $(TMTTF)_2Br$ were prepared using standard electro-chemical procedures [11]. The specific heat was measured between 0.07 K and 7.5 K by a transient heat pulse method as we had already done under similar conditions with many 1D-materials. The sample in the form of a great number of needles ($\sim$ 100) with a weight of 67 mg was smoothly pressed between two silicon plates (2 cm^2 in surface). The thermal contact between needles and the Si plates was improved with the use of 17 mg of Apiezon N grease spread over the Si plates. The heat capacity of addenda measured independently was subtracted. The ratio of heat capacity of the addenda to the total specific heat varied between $\sim$ 50% at $T = 5$–6 K and $\sim$ 45% at $T = 0.5$ K. The duration of the heat pulse was between 0.3 s ($T \sim 0.1$ K) and 2 s ($T \sim 6-7$ K). Thermal transients in response to heat pulses were exponential down to 0.7 K, but a progressive deviation to this law develops at further decreasing T. As previously we adopt the convention to define the specific heat from the initial decay of the transient, that means a minimum value for the time-dependent specific heat [12]. In the case of long heat delivery (up to 10 h), the reference temperature T_0 has to be stabilized within relative fluctuations of $\pm 2 \times 10^{-4}$ in order to get a precise estimation of the integrated energy release towards the thermal bath through the thermal link after switching off the heat source. The present conditions are very similar to those reported previously in the case of $(TMTSF)_2PF_6$ [9, 13]. The method to define the long-time specific heat from the integrated energy release is the same in both cases. Also to be outlined is the good thermal diffusivity of the sample assembly (see Fig. 3): the maximum increment ΔT in response to the heat pulse is reached within only 0.7 s at 90 mK (the duration of the heat pulse itself contributes to 0.3 s). This experimental diffusivity can be compared to the case of $(TMTSF)_2PF_6$ (with a total sample mass of 150 mg where the maximum increment is reached within 1.5 s at 150 mK [13]).

3. Results and Discussion

3.1. Short-Time Scale Specific Heat. — We firstly discuss data obtained in response to heat pulses. In the case of deviation to exponential decay (here, starting at $T \sim 0.7$ K) we adopt the convention as previously done, to define C_p from the initial decay of the transient, which means a minimum value of the time-dependent specific heat [12, 13]. Raw data of the specific heat of $(TMTTF)_2Br$ obtained in this way are reported in Figure 1 between 0.07 K and 2 K. These results are very similar to those obtained for $(TMTSF)_2PF_6$ (two different batches [9,13]). The deviation to the T^3 lattice term which develops below 1 K can be analyzed with a self-consistent analysis with three contributions to C_p:

$$C_p = C_N T^{-2} + aT^{\nu} + \beta T^3,$$

sum of an hyperfine nuclear contribution, the usual low-energy excitations and a regular phonon term.

Best fits to the data below 2 K give possible the numerical values:

$$\begin{aligned} \text{from} \quad C_p &= 0.010 \times T^{-2} + 2.4\ T^{0.4} + 8.0\ T^3 \ (\text{mJ/mol K}) \\ \text{to} \quad C_p &= 0.011 \times T^{-2} + 2.8\ T^{0.5} + 7.6\ T^3. \end{aligned}$$

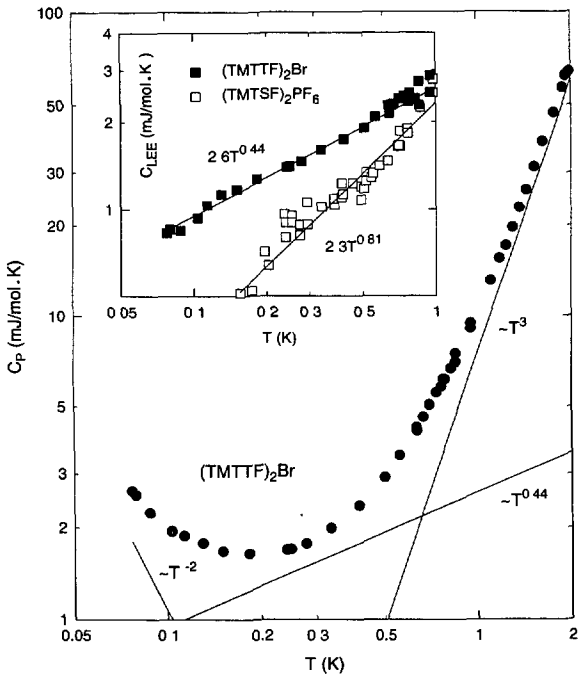

Fig. 1. — The specific heat of $(TMTTF)_2Br$ obtained by the short pulse technique exhibits three different contributions below 2 K: the phonon term, the low-energy excitations contribution and the hyperfine nuclear term. The best fit gives: $C_p = 0.011T^{-2} + 2.6T^{0.44} + 7.8T^3$ mJ/mol K. The LEE contribution, C_{LEE}, is compared to that one of $(TMTSF)_2PF_6$ [13] in the inset.

3.1.1. Hyperfine "Nuclear" Contribution. — The origin of the hyperfine nuclear contribution is still not clear. We reasonably ascribe it to a nuclear hyperfine origin in agreement with this T-range below 0.2 K where occurs the T^{-2} contribution. However, we cannot estimate its absolute amplitude due to the strong time-dependence effects in this range. Our general interpretation is that the observation of nuclear hyperfine levels in these insulating DW systems is allowed by the presence of extra-phonon LEE excitations. In addition, in the case of CDWs, there is obviously a coupling between the slow dynamics of the LEE and the modulation of the electric field gradient at the nuclei which exhibit an electric quadrupolar moment. It is why the same slow dynamics is obeyed in the low T-range, even in the case where the main contribution to C_p is that of the nuclear term in comparison to the LEE (at $T \lesssim 0.15$ K for TaS_3 [12]). In the case of TaS_3, the $C_N T^{-2}$ contribution defined on the pulse time-scale yields a reasonable quadrupolar frequency value for the ^{181}Ta nuclei.

This general interpretation is supported by the comparison of experiments performed on $(TMTSF)_2PF_6$ samples from 2 different batches on one hand, and in our recent results in $(TMTSF)_2AsF_6$ (to be published) on the other hand (despite that the exact origin of the nuclear term is not elucidated; indeed in $(TMTSF)_2PF_6$ a purely quadrupolar electric contribution is not possible since none of the constituent nuclei bears a quadrupolar moment). Between the two $(TMTSF)_2PF_6$ samples (originating from two different batches [9,13]), there is an overall agreement between the amplitudes of C_{LEE} and C_N. On the other hand, the $(TMTSF)_2AsF_6$ sample reveals a surprisingly very small (if any) amplitude of C_{LEE} and in the same time a nuclear term which is reduced by a factor of about 50 in comparison to $(TMTSF)_2PF_6$.

The alternative origin of C_N in the nuclear magnetism due to the local field induced by the SDW seems to be unrealistic in view of the local field distributions measured either by NMR [4,5] or muon spin-rotation experiments [14], which are in the range of hundreds kHz, instead of nuclear frequency of several tens of MHz (on the proton ^1H sites) necessary to interpret our data ([1]).

In $(TMTTF)_2Br$, if we consider the possible mixed SDW-CDW character of the ground state, as recently suggested from X-ray experiments [7,8], a possible quadrupolar electric contribution can originate from the sulphur atoms (in the stack) and from the Br anions, each bearing a quadrupolar moment. The amplitude of C_N is however smaller than in $(TMTSF)_2PF_6$ (with $C_N = 0.16$ and 0.065 mJ/mol K for samples from respective batches [13,9]) by about one order of magnitude.

3.1.2. LEE Contribution. — The self-consistent analysis yields a well defined LEE contribution which follows a power law over more than one decade of temperature, as shown in the inset of Figure 1 with possible parameters:

$$C_{LEE} = 2.4\ T^{0.4} \div 2.8\ T^{0.5}\ (\text{mJ/mol K})$$
$$\text{or} \qquad 40\ T^{0.4} \div 47\ T^{0.5}\ (\text{erg/g K}).$$

This magnitude is comparable to that of the CDW system TaS_3, with similar sub-linear power law coefficient [12]. It corresponds to the upper range of LEE contributions among numerous DW systems [15].

We compare it in the inset of Figure 1 with the LEE contribution of $(TMTSF)_2PF_6$ [13], which exhibits a larger exponent ($\nu \simeq 0.8-1$).

3.1.3. Lattice Contribution. — The above given analysis is consistent with a regular βT^3 law for the lattice contribution for $T \leq 2$ K. In the same way as for $(TMTSF)_2PF_6$, we can relate this low-T phonon term to a usual Debye temperature: $\theta_D^3 = \dfrac{1944}{\beta} \times r$, with β in J/mol K, r is the number of atoms per formula unit ($r = 53$), and the molar mass = 601 g. The value of $\beta = 7.8 \times 10^{-3}$ J/mol K^4 yields $\theta_D = 236$ K, to be compared to 200 K in the case of $(TMTSF)_2PF_6$ compound [13].

In Figure 2, we have extended the analysis up to 7.3 K, the upper limit of available data with this technique. After subtraction from total C_p of $C_N T^{-2}$ and C_{LEE}, we report data between 0.5 and 7.3 K ascribed to vibrational (or configurational) excitations in a C/T^3 diagram, to point out the possible deviation from the Debye behaviour. Data previously obtained in $(TMTSF)_2PF_6$ [13] are also reported in the Figure 2 for comparison.

a) The first apparent feature is the discontinuity at 1.9-2.0 K, common with $(TMTSF)_2PF_6$. The amplitude of the C_p jump is comparable: $\sim 10\%$ in $(TMTTF)_2Br$ compared to $\sim 7\%$ in $(TMTSF)_2PF_6$. We have recently measured a similar jump in $(TMTSF)_2AsF_6$ (to be published). This seems to be a common property of these organic salts and may indicate the existence of sub-phases in the SDW ground state [5,13].

b) For T higher than 2.5 K, there is a rapid increase of C/T^3 up to 7.3 K, but without the characteristic anomaly detected in $(TMTSF)_2PF_6$ around 3-3.5 K ascribed to a glassy-like transition [16-a]. In comparison to the low-T cubic regime, the relative amplitude in C/T^3 at 7 K (near the maximum) is about 2 times larger than in $(TMTSF)_2PF_6$. As, up to now, there are no indication of some other excitations, this extra-contribution should be ascribed

([1]) Nuclear specific heat is $\dfrac{C_N}{R} = \dfrac{1}{3}\left(\dfrac{I+1}{I}\right)\left(\dfrac{\mu_\nu H_{eff}}{k_B}\right)^2$, with $I = 1/2$ the nuclear spin of the proton, μ_ν the proton magnetic moment and H_{eff} a mean local field.

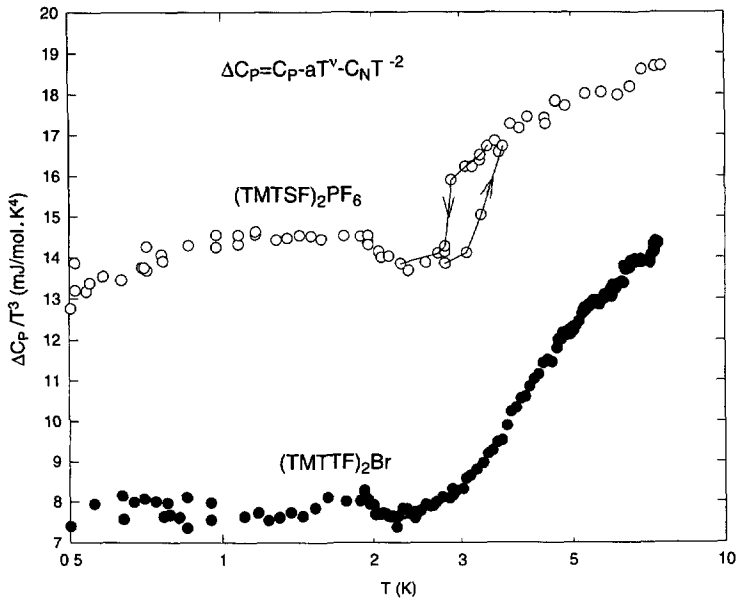

Fig. 2. — Residual, lattice specific heat (after subtraction of the nuclear term and C_{LEE}) divided by T^3 of $(TMTTF)_2Br$ and $(TMTSF)_2PF_6$. Discontinuities at 1.9 K indicate the existence of "sub-SDW" phases coupled to the lattice instabilities in both systems. In the range of the glass transition at 3 K for $(TMTSF)_2PF_6$ (see the manifestation of hysteresis between the first heating run and second cooling run [13]), C_{p} of $(TMTTF)_2Br$ does not show any discontinuity, increasing slowly to the maximum located around 7 K, as measured in both compounds.

to the lattice. There are two possibilities which are not exclusive: the low-lying phonons [18] and the configurational entropy [17], related to the disorder character of pinned DW. This fact raises the actual and important question of the role of electron-phonon coupling in the SDW stabilization.

The configurational approach is additionally supported by the fact that in the temperature range of the peak in C_{p}/T^3, the specific heat of $(TMTTF)_2Br$ appears to be sensitive to the kinetics of the relaxation (similarly to a measurement of C_{p} at different frequencies). Indeed, measurements performed on the same sample by another transient heat pulse technique (in another cryostat), on a much shorter time scale [18], give a specific heat lower by ~ 20 to 40% between 2.5 and 7 K; the bump in C_{p}/T^3 is actually centered at 7 K and the SDW transition is detected at $T_{\mathrm{SDW}} = 11.7$ K, with a relative amplitude of less than 1% of total C_{p} [18].

The frequency dependence of C_{p} in the same temperature range is also confirmed in the case of $(TMTSF)_2PF_6$, measured by four different techniques, from quasi-adiabatic to the a.c. one, where the configurational interpretation of the C/T^3 bump (at least a part of it) was naturally involved due to the existing glass transition [17].

3.2. Long Time Heat Relaxation. — As indicated in the Introduction, the first direct evidence of a time-dependence $C_{\mathrm{p}}(t)$ below 1 K is given by the deviation to an exponential decay of the transients after a heat-pulse. This feature occurs progressively below 0.7 K, like in $(TMTSF)_2PF_6$ [9], but the dynamics observed is very different. Whereas for $(TMTSF)_2PF_6$, except for the initial part (the time span of a few seconds, similarly as for $(TMTTF)_2Br$ shown

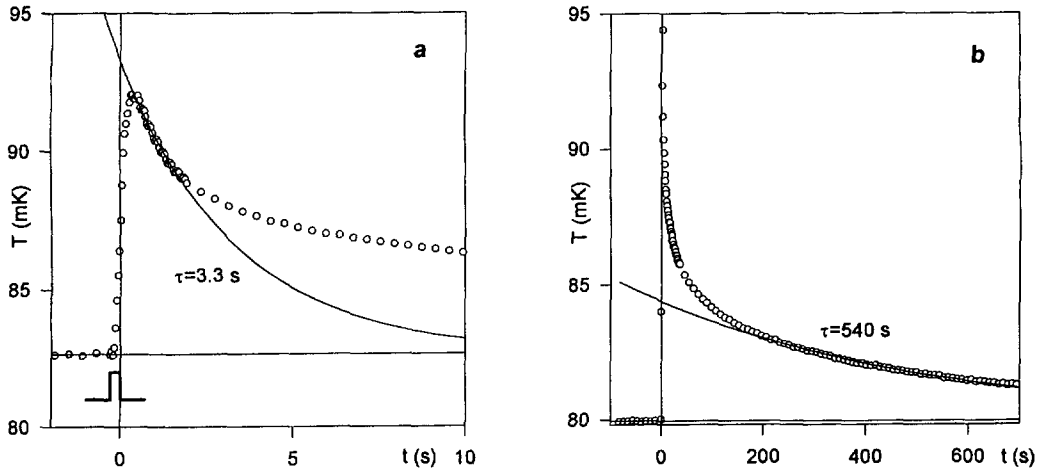

Fig. 3. — The decay of the temperature increment ΔT in $(TMTTF)_2Br$ at $T \simeq 85$ mK after a heat pulse and the illustration of the determination of short-time and long-time C_p. a) Heat transient at $\bar{T} = 88$ mK after the heat pulse of 0.3 s with the amplitude $\Delta T/T_0 = 12\%$. We verify a very good thermal diffusivity of our sample (the maximum ΔT has been reached within 0.7 s). The short-time C_p is deduced from the initial part of the decay (a few seconds) fitted by an exponential with the corresponding $\tau = 3.3$ s. b) Characteristic heat transient at $\bar{T} = 82.2$ mK taken for the estimation of long-time C_p after the heat pulse of 1 s recorded in much longer time span, over 10 minutes. The corresponding amplitude and time constant of the exponential fit to the long-time tail are $\frac{\Delta T}{T_0} = 5.5\%$ and $\tau = 540$ s.

in Fig. 3a), it is not possible to fit any part of the transient by an exponential decay at low temperatures, in the case of $(TMTTF)_2Br$ this is possible for the final part of the relaxation, down to the lowest T (over a time span typically of 10 minutes, as shown in Fig. 3b). It allows us to extract two limiting values of C_p: the first one defined by the initial decay (Fig. 3a), the second one by the long-time span, corresponding to a maximum value of C_p. The latter one is defined in the usual way: *i.e.* by the extrapolation of the exponential law to the "time origin" of the temperature decay. We note that within this procedure C_p is calculated from the "ideal" ΔT jump, estimated at $t = 0$. From the time constant τ and the heat capacity values, we can extract the thermal link $R_\ell = \frac{\tau}{mC_p}$. This value agrees within about 30% (it is systematically smaller) with the value defined in the steady state equilibrium conditions, obtained during very long energy delivery over a few hours. In the case of $(TMTSF)_2PF_6$, such a determination of R_f from the transient regime was absolutely impossible, for any time scale at least up to ~ 20 minutes. We have to outline the huge difference in the time scales in Figures 3a and 3b, by a factor of 70, and the fact that it is impossible to fit by an exponential law the intermediate regime between 1 s and the final long exponential tail, in any significant time interval.

3.2.1. Schottky Anomaly. — In Figure 4 we report C_p data obtained in these two extreme time-spans. The two curves are totally different; for the long-time span, C_p shows a minimum at 0.5 K and at lower T an anomaly with a well-defined maximum at 110-120 mK, which is in a good agreement between 80 mK and 0.3 K with a Schottky anomaly. The agreement can

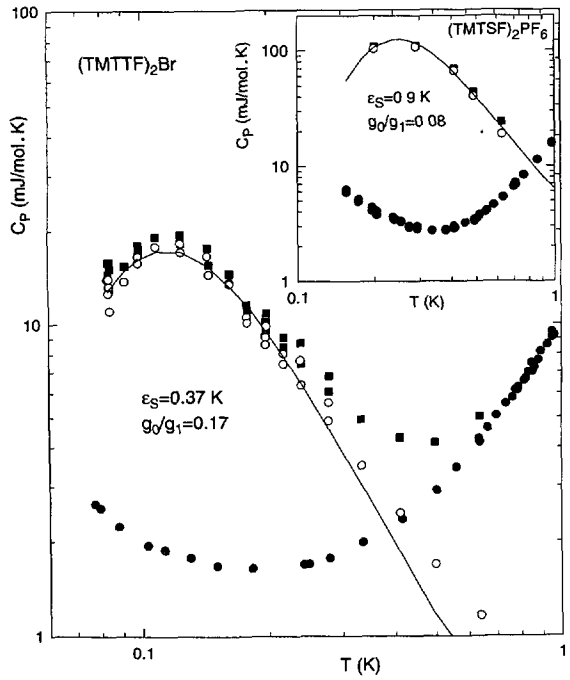

Fig. 4. — Long-time specific heat (■), defined as explained in Figure 3b, compared with the short-time determination (•) of $(TMTTF)_2Br$. The anomaly which remains after subtraction of the short-time specific heat (○) can be fitted to a Schottky anomaly with the maximum $C_{p_{max}} = 18$ mJ/mol K at $T_m = 0.11$ K, with a splitting $\varepsilon_s = 0.37$ K and the ratio of degeneracy $g_1/g_0 \simeq 6$. For comparison we also show in the inset a similar anomaly obtained for $(TMTSF)_2PF_6$ (batch of Ref. [13], unpublished) defined in the same way, with $\varepsilon_s = 0.9$ K and $g_1/g_0 \simeq 12$. The full lines represent the corresponding fits.

be extended up to 0.5 K after subtraction of the short-time contribution ([2]). Supposing the simple case, as instructive one: the system consisting of two levels, the ground state and one higher level, we obtain that the corresponding energy splitting should be $\varepsilon_s = 0.37$ K with the ratio of degeneracy $g_1/g_0 \cong 6$.

This anomaly determined on the long-time span is also observed in the case of the $(TMTSF)_2PF_6$ salt (inset of Fig. 4). But in that case, the C_p determination was done by the integration of total heat release, in the regime of saturation (thermodynamical equilibrium) when the energy relaxation does not depend anymore on the time during which the thermal flow has been applied. The same kind of measurements have also been done for $(TMTTF)_2Br$, in which the equilibrium state has been achieved at much shorter "waiting times" than for $(TMTSF)_2PF_6$ (see the following chapter). However, we found some difference between these two determinations, 40% at maximum, with no evidence for a maximum of a Schottky anomaly in C_p obtained by the integration method. We have no explanation for these differences

([2]) Here we have to point out the consistency of the determination of C_{LEE} on the short time scale. Although the origin of $C_N T^{-2}$ contribution in non-equilibrium conditions, as defined in paragraph 3.1, is not clarified, the estimation of C_{LEE} seems to be undoubtful. The same contribution persists in the conditions of the thermodynamic equilibrium together with the Schottky anomaly and the lattice term.

except the decoupled channels of relaxation to the thermal bath for different excitations giving rise to the smaller effective thermal link than that one related to the final thermodynamical equilibrium of the whole system.

Nevertheless we can compare the position and the amplitude of the Schottky anomalies in both systems, as shown in Figure 4. The maximum of the anomaly in $(TMTTF)_2Br$, $C_{p_{max}} = 18$ mJ/mol K, is about seven times smaller than for $(TMTSF)_2PF_6$. The maximum in $(TMTSF)_2PF_6$ appears at $T_{max} \simeq 0.25$ K with $C_{p_{max}} = 120$ mJ/mol K. The best fit yields a splitting $\varepsilon_s = 0.90$ K with the ratio of degeneracy $g_1/g_0 = 12$. So high ratios of degeneracy obtained for both systems in the usual Schottky anomaly approach are quite unexpected. It suggests the existence of a distribution of energy levels and it demands more sophisticated treatment. In the case of $(TMTSF)_2PF_6$ the energy levels have been ascribed to specific metastable states due to the strong-pinning phenomenon at the pinning centers located close to regions of commensurability [19]. Certainly, it should be reexamined in the case of $(TMTTF)_2Br$ which is "nominally" commensurate.

3.2.2. "Pumping Time" Effects (Aging Effect). — In previous studies on several CDW compounds and the SDW system $(TMTSF)_2PF_6$, we have brought evidence for a strong dependence of the thermal transients, and consequently the C_p values, on the duration of energy delivery ("pumping" time). Such effects we named "aging" and "waiting time" dependence. They were particularly evident in the case of TaS_3 (CDW) [10] and $(TMTSF)_2PF_6$ (SDW) [9, 16b]. Let us briefly summarize them:

(i) Aging: on increasing the duration of the energy supply, for the same temperature increment ΔT_0, from pulses of 1 s or less, up to t_w of more than 10 h, the corresponding relaxation rate $\partial \Delta T(t)/\partial \log t$, proportional to the distribution of relaxation times $g(\tau)$, is shifted to longer times.

(ii) Saturation of aging effect (interrupted aging): for very long t_w (10 h at 0.1 K for either TaS_3 or $(TMTSF)_2PF_6$), that we correlate to the achievement of the thermodynamical equilibrium, the aging stops.

(iii) Broad spectrum $g(\tau)$: it extends over several decades of the time scale and depends on the temperature.

These features, except for (iii) (the characteristics of $g(\tau)$), are represented in Figure 5 for $(TMTTF)_2Br$. Because of the large-time span, the transients $\Delta T(t)$ and their logarithmic derivatives (proportional to $g(\log \tau)$) are shown on log-scales for three "pumping" times and for two-representative temperatures: one at $T = 130$ mK exhibiting large time dependent effects, the other at $T = 770$ mK where the time effect has almost disappeared. Nevertheless it is still possible to deduce that even at 0.77 K the system continues to evolve up to 20 s, but that for 10 minutes the thermodynamical equilibrium is certainly reached.

However, the main differences in comparison to previously observed dynamical effects in $(TMTSF)_2PF_6$ appear for the lowest temperatures (Fig. 5a). It seems that there is no broad distribution $g(\log \tau)$ which moves on the time scale with the waiting time (as in the real aging effect) and stops when the equilibrium time t_e is reached as observed for $(TMTSF)_2PF_6$ [16b] and TaS_3 [10]. The dynamics of energy relaxation in $(TMTTF)_2Br$ reveals almost "discrete bands" of the relaxation time, or better to say, successive narrower distributions of relaxation times. For shorter pulses (up to a few seconds) the relaxation rate is very broad and exhibits a fine, "discrete" structure as for a manifold of narrower distributions. For longer durations of heat input, most of the weight is moved to the distribution centered at longer time (200-400 s).

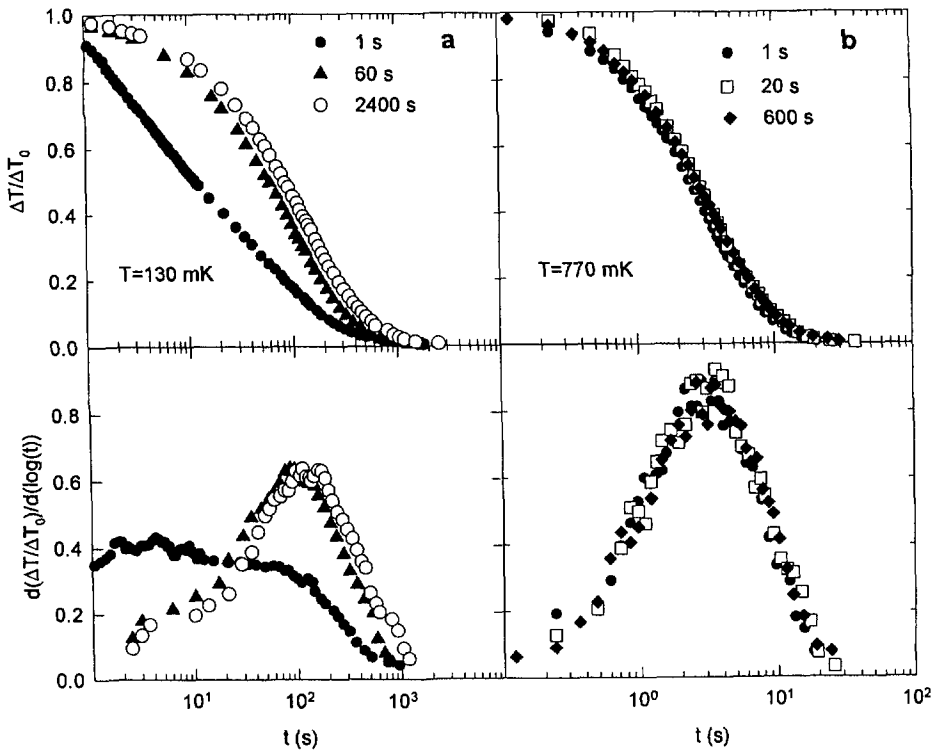

Fig. 5. — The variation of $\Delta T(t)/\Delta T_0$ and the corresponding relaxation rate $\dfrac{\mathrm{d}(\Delta T(t)/\Delta T_0)}{\mathrm{d}\log t}$ as a function of time in a semi-log plot for different duration of heat delivery at two temperatures ($T = 130$ mK (a) and $T = 770$ mK (b)) show a specific time-dependent effect which disappears at higher T. The relaxation rates (lower curves) which represent the distribution of the relaxation times, demonstrate the existence of successive distributions for shorter duration of pulses (shorter pumping time) at lower T. The distribution for long pumping time is almost two times narrower than for $(TMTSF)_2PF_6$ in similar conditions ($T = 0.2$ K [16b]).

This is also the main reason why in this case we rather prefer to use the term "pumping time" instead of waiting time.

Distribution of relaxation times for $(TMTSF)_2PF_6$ is more than two times broader than for $(TMTTF)_2Br$ at $T \approx 200$ mK: that may be the reason for a very complex, glassy relaxation, consistent with the existence of the glass transition at 3 K. This I-SDW system demonstrates a very subtle interplay with a $2k_F$ CDW [7,8]. Due to proximity to the commensurate state and the mixture of the ground states, it exhibits a highly frustrated state with typical glassy relaxation. On the other side, $(TMTTF)_2Br$ exhibits C-SDW. The successive distributions separated by decades in time observed in $(TMTTF)_2Br$ and represented in Figure 5a are probably the manifestation of different relaxations as for instance commensurate domains and domain walls between them. The distribution of corresponding relaxation times is not a large one. The width is almost Debye-like (width at half maximum: $W_D = 1.14$ decade) at 1 K, and it increases slightly at lower T, reaching $W \approx 1.5W_D$ below 100 mK. This explains the possibility to fit the direct signal $\Delta T(t)$ in response to the heat pulse by an exponential decay over the time scale 200-600 s (Fig. 3b).

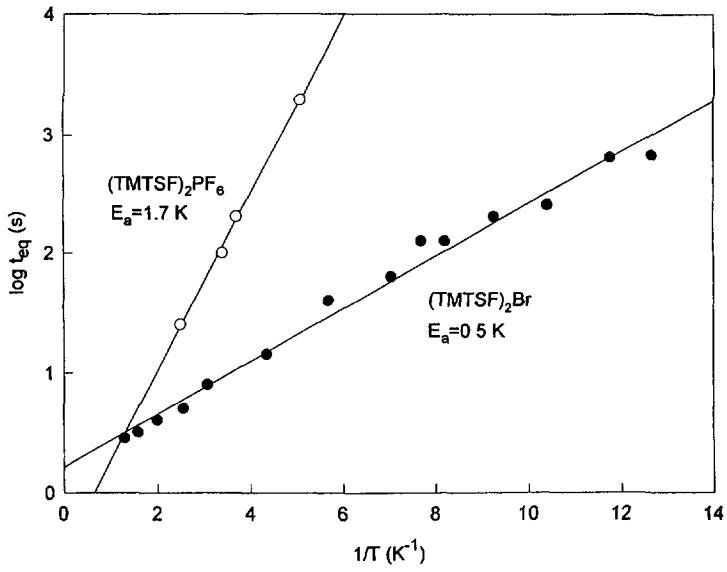

Fig. 6. — Variation of the time t_{eq}. necessary for the system to reach the thermodynamic equilibrium (*i.e.* the pumping time when the time-dependent effect explained in Fig. 5 saturates), reported in an Arrhenius plot. The underlying relaxational processes in both systems, $(TMTTF)_2Br$ and $(TMTSF)_2PF_6$ are thermally activated. An activation energy $E_a = 0.5$ K for $(TMTTF)_2Br$ allows the thermal equilibrium at $T = 0.1$ K to be reached within a few minutes. For $(TMTSF)_2PF_6$ one should wait for weeks.

The most dominant long time process shows the aging effect and the temperature dependence of the equilibrium relaxation time — when the aging is interrupted — reflects the activated mechanism of the underlying relaxation ($\tau = \tau_0 \exp(E_a/kT)$) with an activation energy $E_a = 0.5$ K. It is represented together with the results previously obtained for $(TMTSF)_2PF_6$ in Figure 6. It is worth mentioning that the ratio of the activation energies for both systems $E_{a_1}/E_{a_2} \approx 3$ is approximately the same as the ratio of the energy splitting of the corresponding Schottky anomalies. Attempt microscopic time for the Arrhenius behavior, τ_0, is of the order of one second. Because the activation energy of the mean relaxational process is a few times smaller, the thermodynamical equilibrium for $(TMTTF)_2Br$ can be reached at 0.1 K within less than 5 minutes, but for $(TMTSF)_2PF_6$ one should wait two weeks! Experimentally this has been verified, because it was necessary to spend 4 days for cooling the sample down to 0.12 K from only slightly higher temperature ($T_i \approx 0.160$ mK).

4. Conclusions

Our thermodynamical investigation of C-SDW system $(TMTTF)_2Br$ gives some new and very important informations on its low-temperature ground state between 0.07 and 7 K. It is not an uniform ground state. First of all, there is a discontinuity in C/T^3 at 1.9-2 K, as has been found previously in $(TMTSF)_2PF_6$ and recently in $(TMTSF)_2AsF_6$. This looks like to be a common feature of this family and has been interpreted in the case of $(TMTSF)_2PF_6$ as a sub-SDW transition [13]. Although $(TMTTF)_2Br$ does not exhibit a glass transition as $(TMTSF)_2PF_6$ at 3 K, it shows evidence of a substantial configurational contribution,

a characteristics of a disordered ground state. This latter feature is related to the underlying lattice and is the consequence of the existing electron-phonon interaction. These conclusions are strongly supported by new evidences of the interplay of SDW-CDW in both compounds [7, 8].

Below 1 K, the measured specific heat exhibits all features as found previously for DW systems. In addition to the usual phonon term two other contributions appear, an hyperfine "nuclear" term and the contribution from low-energy excitations. Because of the long relaxation time of these excitations the specific heat is time-dependent. Long-living excitations give rise to an anomaly of a Schottky type located at $T_{max} = 0.110$ K. We believe that it is of the similar microscopic origin as the much larger one found in $(TMTSF)_2PF_6$ [19]. It seems that the ground state is not perfectly commensurate. The experimental conditions concerning possible pressure effects (pressure induced by the Si-plates in the sample arrangement and rigidification of silicon grease) may affect the strictly commensurate ground state [6]. It was shown [19] that new metastable states are formed at the strong pinning centers located close to the regions of commensurability and they are the consequence of the induced plastic deformations of DW. However, there are significant differences in the dynamics of their relaxation. For $(TMTSF)_2PF_6$, consistent with existence of a glass transition, the dynamics has all the characteristics of a glass with a very large distribution of relaxation times. In the case of $(TMTTF)_2Br$ the dynamics of the energy relaxation shows some discrete structure with separated distributions of relaxation times indicating probably different processes, as for domains and domains walls between them or discommensurations.

It is worthwhile mentioning recent theoretical results which are on the lines of our reasoning. Namely the main argument against the existence of a new phase in the Peierls DW state was taken from the theoretical considerations of the random-field XY model, since the commonly used Fukuyama-Lee-Rice model for an elastically deformable CDW pinned by random impurities is similar to that one [20]. It has been believed that these systems are simply disordered at low temperatures, possessing many metastable states, with no new phase transition at $T_c \neq 0$. Recently this intriguing question — can phases exist which exhibit some kind of topological or other type of order that distinguishes them from the high T disordered phase? — got its positive answer. There are numerical and analytical evidences for the existence of a phase transition to an equilibrium elastic glassy phase in a 3D weak random XY magnets. In this picture the domain walls turn out to be the natural objects at long length scales [21]. Although the arguments given for XY random field magnets should apply also for 3D vortex lattices in dirty types-II superconductors, analogous phases can exist also in DW systems.

Acknowledgments

We acknowledge the analysis of the transients made by the students A. Kiš and D. Pavičić. This work has been realized in the frames of the bilateral cooperation between CRTBT-CNRS and Institute of Physics.

References

[1] Ishiguro T. and Yamaji K., in "Organic Superconductors" (Springer-Verlag, Berlin, 1990).
[2] Jérome D., in "Organic Conductors: Fundamental and Applications", Farges J.P., Eds. (M. Dekker, New York 1994) p. 405.

[3] Bourbonnais C., in "Highly Correlated Fermion Systems and High T_c Superconductors", Douçot B. and Rammal R., Eds. (1994).
[4] Barthel E., Quiron G., Wzietek P., Jérome D., Christensen J.B., Jørgensen M. and Bechgaard K., *Europhys. Lett.* **21** (1993) 87.
[5] Takahashi T., Maniwa Y., Kawamura H. and Saito G., *Physica* **143B** (1986) 417.
[6] Klemme B.J., Brown S.E., Wzietek P., Kriza G., Batail P., Jérome D. and Fabre J.M., *Phys. Rev. Lett.* **75** (1995) 2408.
[7] Pouget J.P. and Ravy S., *J. Phys. I France* **6** (1996) 1501.
[8] Pouget J.P. and Ravy S., *Synthetic Metals* (1997) in press.
[9] Lasjaunias J.C., Biljaković K. and Monceau P., *Phys. Rev. B* **53** (1996) 7699 and references therein.
[10] Biljaković K., Lasjaunias J.C., Monceau P. and Levy F., *Phys. Rev. Lett.* **62** (1989) 1512.
[11] Delhaes P., Coulon C., Amiell J., Flandrois S., Torreilles E., Fabre J.M. and Giral L., *Mol. Cryst. Liq. Cryst.* **50** (1979) 43.
[12] Biljaković K., Lasjaunias J.C., Monceau P. and Levy F., *Europhys. Lett.* **8** (1989) 771.
[13] Lasjaunias J.C., Biljaković K., Monceau P. and Bechgaard K., *Solid State Commun.* **84** (1992) 297.
[14] Le L.P. *et al.*, *Europhys. Lett.* **15** (1991) 547.
[15] Lasjaunias J.C., Biljaković K. and Monceau P., *Physica B* **165 and 166** (1990) 893.
[16] a) Lasjaunias J.C., Biljaković K., Nad' F., Monceau P. and Bechgaard K., *Phys. Rev. Lett.* **72** (1994) 1283; b) Biljaković K., Nad' F., Lasjaunias J.C., Monceau P. and Bechgaard K., *J. Phys.: Condens. Matter* **6** (1994) L135.
[17] Odin J., Lasjaunias J.C., Biljaković K., Monceau P. and Bechgaard K., *Solid State Commun.* **91** (1994) 523.
[18] Yang Hongshun, Lasjaunias J.C. and Monceau P. (to be published).
[19] Ovchinnikov Yu. N., Biljaković K., Lasjaunias J.C. and Monceau P., *Europhys. Lett.* **34** (1996) 645.
[20] Littlewood P.B. and Rammal R., *Phys. Rev. B* **38** (1988) 2675.
[21] Fisher D.S., *Phys. Rev. Lett.* **78** (1997) 1964.